



Positive correlation between renal tubular flattening and renal tubular injury/interstitial fibrosis in murine kidney disease models

Yuki TAKAHASHI¹⁾, Masaki WATANABE¹⁾, Koki HIURA¹⁾, Ai ISOBE¹⁾, Hayato SASAKI¹⁾ and Nobuya SASAKI¹⁾*

¹⁾Laboratory of Laboratory Animal Science and Medicine, School of Veterinary Medicine, Kitasato University, Towada, Aomori 034-8628, Japan

ABSTRACT. The number of patients with chronic kidney disease (CKD) is growing continuously globally. In order to study pathogenesis and mechanisms, many animal models have been developed, including spontaneous, genetic, and induced models. Although each type of CKD shows disease-specific tissue changes in the early stages, tubular disorder and interstitial fibrosis histologically occur in the course of progression to end-stage renal failure. Therefore, the quantification of tubular disorder and interstitial fibrosis in CKD research using animal models is essential for measuring the degree of CKD severity and, thus, efficacy of therapeutic agents. Several strategies have been used to quantify interstitial fibrosis. Among scoring factors, renal tubular flattening can be quantitatively evaluated easily and inexpensively. However, the diagnostic value of renal tubular flattening evaluation has not been investigated previously. Therefore, in this study, we investigated the correlation between renal tubular flattening and interstitial fibrosis or renal tubular injury markers. We observed a strong correlation between the degree of tubular injury/interstitial fibrosis and renal tubular flattening in three types of mouse renal disease model. This is advantageous because rapidly advancing technologies such as artificial intelligence and image processing can be easily applied; hence, a more precise, objective, and quantitative diagnosis should be possible in the future.

KEY WORDS: interstitial fibrosis, murine kidney disease models, renal tubular flattening, renal tubular injury

J. Vet. Med. Sci.

83(3): 397–402, 2021

doi: 10.1292/jvms.20-0692

Received: 8 December 2020

Accepted: 25 December 2020

Advanced Epub:

10 January 2021

Patients with chronic kidney disease (CKD) show symptoms of proteinuria or a prolonged (more than three months) decrease in glomerular filtration rate [15]. This disease is categorized in the high-risk group of patients with end-stage renal failure. The number of patients with CKD is growing continuously globally. When CKD progresses, it leads to end-stage renal failure, which requires dialytic treatment that costs a vast amount, leading to an increase in medical expenditure [14]. Therefore, the development of novel markers for monitoring the onset and progression of CKD and the establishment of novel treatment methods are urgently needed. Common causes of CKD include diabetes, high blood pressure, glomerular disease, and other CKD risk factors. Although each type of CKD shows disease-specific tissue changes in the early stages, tubular disorder and interstitial fibrosis histologically occur in the course of progression to end-stage renal failure. Renal fibrosis is tissue change that mainly associated with CKD-related tubular disorder and interstitial fibrosis and is considered a significant treatment target to prevent progression to end-stage renal failure [25]. Therefore, the quantification of tubular disorder and interstitial fibrosis in CKD research using animal models is essential for measuring the degree of CKD severity and, thus, efficacy of therapeutic agents. Several strategies have been used to quantify interstitial fibrosis, including Sirius red staining or Masson's trichrome staining to quantify fibrillization regions, tubular disorder scoring for morphological analysis of renal tubules, and various injury markers, such as α -SMA, neutrophil gelatinase-associated lipocalin (NGAL), L-FABP, and Kim-1 [6, 7, 9, 10, 16, 23]. The tubular disorder score includes flattening, expansion, degeneration, atrophy, and brush border loss of renal tubules [27]. Among these scoring factors, renal tubular flattening (decrease in height) can be quantitatively evaluated easily and inexpensively [1–3, 19, 20]. However, the diagnostic value of renal tubular flattening evaluation has not been investigated previously. Therefore, we analyzed the correlation between the degree of interstitial fibrosis and renal tubular flattening in kidney disease.

*Correspondence to: Sasaki, N.: nobsasa@vmas.kitasato-u.ac.jp

©2021 The Japanese Society of Veterinary Science



This is an open-access article distributed under the terms of the Creative Commons Attribution Non-Commercial No Derivatives (by-nc-nd) License. (CC-BY-NC-ND 4.0: <https://creativecommons.org/licenses/by-nc-nd/4.0/>)

MATERIALS AND METHODS

Ethical statement

All animal experiments were approved by the President of Kitasato University, following consideration by the Institutional Animal Care and Use Committee of Kitasato University (Approval ID: No. 19-153,19-154, 19-155). Male FVB/NJcl (FVB) and BALB/cAJcl (BALB/c) mice were obtained from CLEA (Tokyo, Japan). All mice were maintained under the specific pathogen-free conditions. They were given access to sterile food and water *ad libitum* before and during experiments.

Animals

Tns2^{nph} model: FVB-*Tns2^{nph}* mutant mouse (FVB-*nph*) were used as CKD model as described in [22]. Ischemia-reperfusion model (IR): The IR model is created was performed as described previously [18]. Eight-week-old mice (Male FVB) were anesthetized by inhalation of isoflurane and the left kidneys of which were removed, then muscle layer and fascia were closed by using absorbable suture. After ten days of recovery, mice were anesthetized by intraperitoneal injection of the combination of anesthesia drugs as described previously [11], their renal arteries and veins were maintained in an ischemic state with artery clamps (TKS-1-40, BEAR Medic, Ibaraki, Japan) for 30 and 60 min, respectively, then muscle layer and fascia were closed by using absorbable suture. In addition, control mice that underwent sham surgery were subjected to open surgery without clamps. After that, all mice were euthanized by inhalation of an overdose of isoflurane (Escain, Pfizer Japan Inc., Tokyo, Japan) to perform the sample collection. The kidneys were removed 24 hr after replication of ischemia. Adriamycin (ADR) -induced nephropathy model: nephropathy model: BALB/c mice aged eight weeks were administered either ADR (FUJIFILM Wako Pure Chemical Co., Ltd., Osaka, Japan) (10 mg/kg) or saline solution (vehicle group) via the tail vein to evaluate their renal disorder histologically at 14 days after administration.

Histology

Mice Kidneys were fixed with 4% paraformaldehyde (PFA) at 4°C overnight. Kidney blocks were sliced at 2 µm (for Periodic Acid- Schiff (PAS) staining) and 4 µm (for Picro-Sirius Red staining). For renal tubular height measurement, the cortex sides of Kidney sections were photographed randomly in four different views (×100). Two independent researchers blindly measured the renal tubular height in all views to calculate the mean height of each subject. For the subjects with uneven tubular heights, measurements of two to five locations were selected per tubule to obtain the mean value (Fig. 1A). Approximately 700 tubular height measurements were obtained per subject using the aforementioned procedure to calculate the mean value for each subject. For Sirius Red staining, slides were deparaffinized and stained 1 hr with Sirius red in saturated aqueous picric acid and washed with 0.5% acetic acid. To score fibrillization areas using Sirius red staining, the target areas were photographed randomly in eight views (×100), and the positive areas were quantified using ImageJ (<https://imagej.nih.gov/ij/>) to calculate their occupancy rate with respect to the total area. Glomeruli stained with Sirius red and blood vessels were excluded from the calculation.

Immunohistochemistry staining

Kidney sections (5 µm) were deparaffinized and subjected to antigen retrieval in citrate buffer, at 121°C for 15 min. after washing with Tris-buffered saline (TBS), Kidney sections were sealed with 0.3% hydrogen peroxide/methanol for 20 min, and then incubated overnight at 4°C with anti-NGAL antibody (Abcam, Cambridge, UK). Sections were washed with TBS and then incubated with secondary antibody (Histofine SimpleStain MAX PO (Rabbit), Nichirei Biosciences Inc., Tokyo, Japan) for 30 min at room temperature. After washing with TBS, the sections were incubated with 3,3'-diaminobenzidine (DAB) (Wako Pure Chemical Industries Ltd., Osaka, Japan) and hematoxylin at room temperature. To score tubular disorder via immunohistochemistry staining using an anti-NGAL antibody, tissue samples were photographed randomly in eight views (×100), and the areas of DAB staining were quantified using ImageJ to calculate their occupancy rate with respect to the total area.

Statistics

Data was presented as mean ± standard deviation. Student's *t*-test was used to test for significant differences between two groups, and Bonferroni's multigroup test was used to test for multiple groups. *P* value <0.05 was statistically significant. Bonferroni's multigroup test was carried out using GraphPad Prism 5 software (MDF, Tokyo, Japan).

RESULTS

As mentioned above, the quantification of the interstitial fibrotic areas using Sirius red staining should be the standard evaluation method for tubular disorders in patients with kidney disease or in kidney disease models. Thus, for the quantification of tubular disorder and interstitial fibrosis using animal CKD murine model, we used FVB-*Tns2^{nph}* mutant mouse (FVB-*nph*), which is a CKD animal model that exhibits many symptoms of human CKD that progresses gradually over an extended period, including the genetic onset of glomerulosclerosis from birth, fibrillization of tubulointerstitium, renal anemia, and renal failure [17, 21, 22]. The FVB-*nph* mouse reproduces the typical symptoms observed in human CKD progression. In this study, we introduced the *nph* mutation into FVB lines susceptible to nephropathy. The FVB-*nph* group showed more tubular flattening than the WT group, based on the worsening of fibrillization of the interstitium in the renal tubules (Fig. 1B–D). Linear regression analysis indicated a significant opposite correlation between the tubular height and degree of interstitial fibrosis ($R^2=0.7086$; $P=0.0023$) (Fig. 1E).

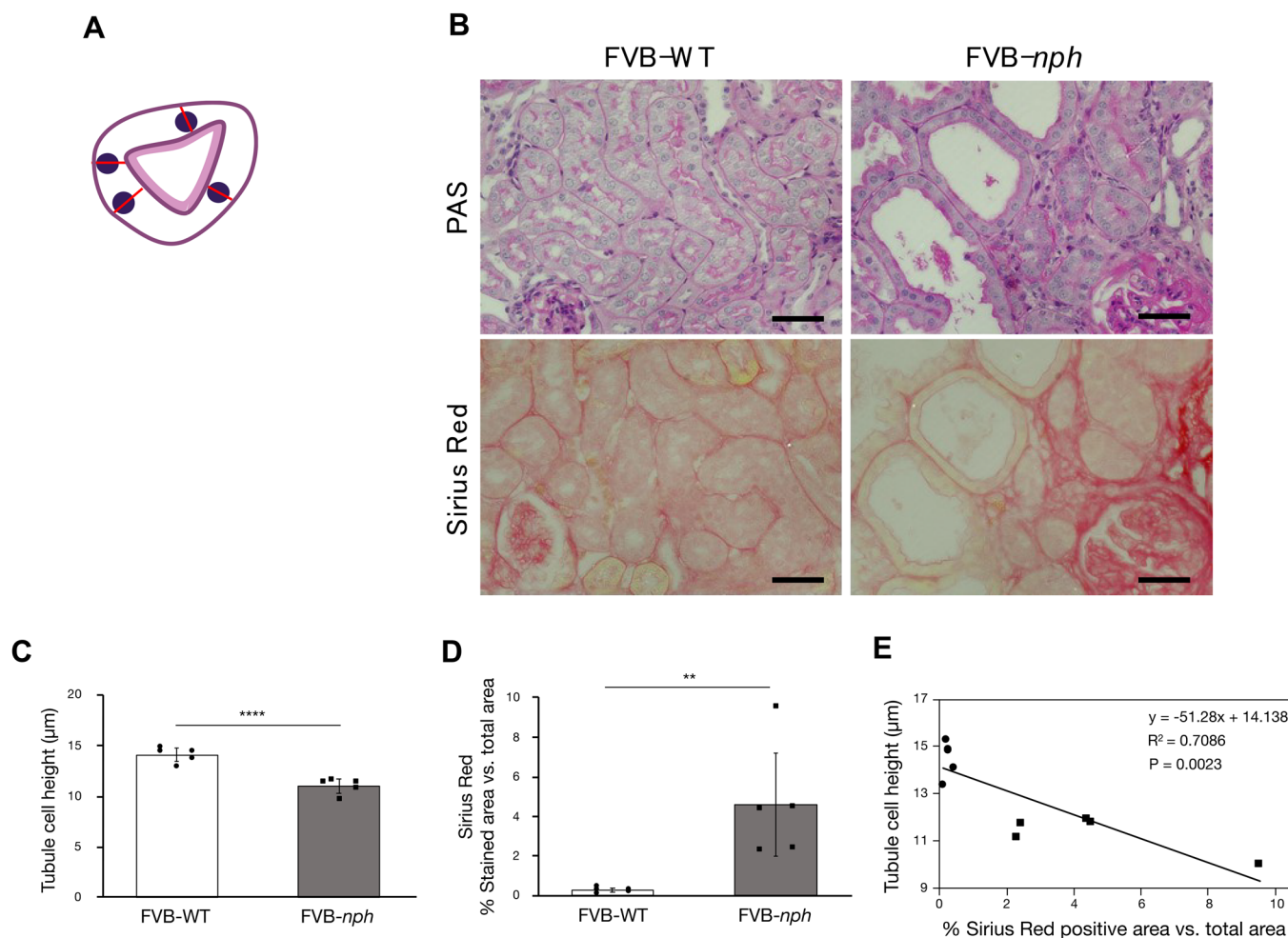


Fig. 1. (A) Measurement of tubular epithelial cell height. Red bars indicate tubule height. (B) Representative images of Periodic Acid- Schiff (PAS) staining and Sirius Red-stained images of 10-week-old FVB-*Tns2^{WT}* (FVB-WT) (left panel) and FVB-*Tns2^{nph}* mutant mouse (FVB-*nph*) (right panel) kidney sections. Upper panel represents PAS-stained images, and lower panel represents Sirius Red-stained images. Scale bars: 50 µm. (C) Graph comparing the tubular heights of FVB-WT and FVB-*nph*. (D) Graph comparing Fibrosis area vs. total area. Data are expressed as mean ± standard deviation; *P*-values were calculated by Student's *t*-test. (E) Scatter plots with liner regression show correlation analysis between the height of tubules height and the degree of the fibrosis score. The linear regression line showed an inverse correlation between tubular height and fibrosis area. Correlation coefficients *R* and *P* values are shown. Black circles indicate the FVB-WT (*n*=5) group, and black squares indicate the FVB-*nph* (*n*=5) group. ***P*<0.01, *****P*<0.0001

Renal tubular injuries and tubular heights were measured using the acute kidney injury (AKI) model—that is, the IR model [5, 12, 18]. Although interstitial fibrosis should not be observed in most AKI cases, including renal ischemic disorder, NGAL expression increased in renal tubular cells [7]. In addition, NGAL is known to be involved in the progression of AKI to CKD and has been proposed as a vital factor in both. Therefore, we demonstrated that NGAL expression correlated with renal tubular height using the IR model. It has been reported that ischemia time is often set at 20 to 60 min and that tubular injury worsens with increasing ischemia time [4, 5, 12, 18]. In this study, mice were subjected to ischemia for 30 min as weak tubular injury and 60 min as strong tubular injury. Increased NGAL expression and tubular flattening were observed in the 30 and 60 min groups. The increase in NGAL expression and flattening of the tubules was more pronounced in the 60 min group because it had suffered more injury (Fig. 2A–C). A decrease in tubular height and an increase in NGAL expression were demonstrated based on an increase in the ischemic state duration (Fig. 2A–C). Linear regression analysis of the results also indicated a negative correlation between renal tubular height and NGAL expression ($R^2=0.6266$, $P=0.011$) (Fig. 2D).

The ADR nephropathy model is often used in kidney disease research because it produces glomerular injuries and minor tubular disorders with a high level of reproducibility using a single dose of ADR [13]. The ADR nephropathy mouse model was used in this study to evaluate renal tubular injuries and heights. Rodent model of ADR-induced nephropathy is often used to explicate the mechanisms of focal glomerulosclerosis (FSGS) and CKD. A single dose of ADR can cause loss of podocytes, persistent proteinuria, and FSGS. Among different mouse strains, BALB/c is sensitive to ADR, whereas C57BL/6 (B6) is resistant. Thus, we used BALB/c in this ADR experiment. In ADR nephropathy, renal interstitial fibrosis, which is a typical finding of CKD, is

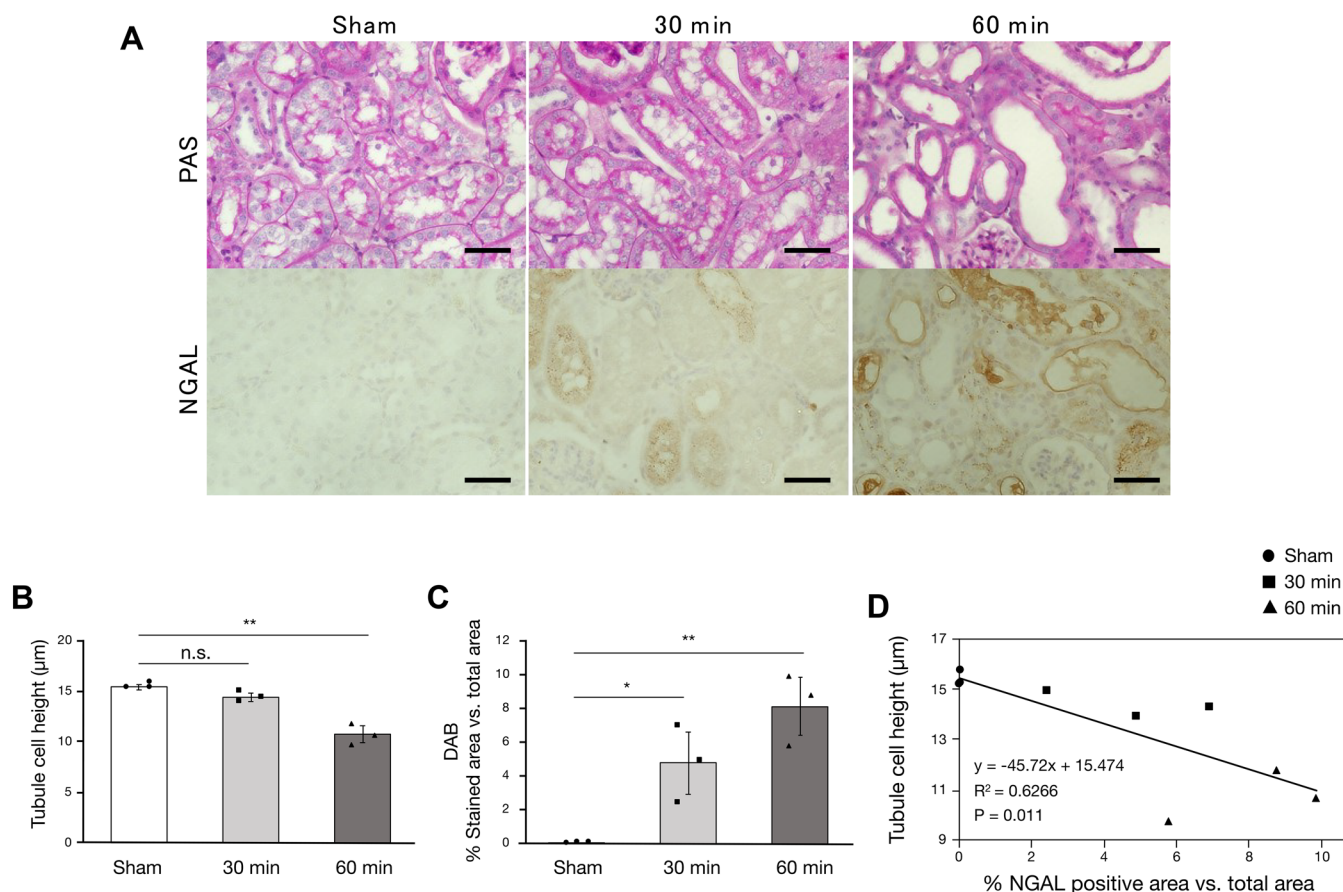


Fig. 2. (A) Representative images of Periodic Acid- Schiff (PAS) staining and immunochemical-stained images with anti- neutrophil gelatinase-associated lipocalin (NGAL) antibody of sham (left panel), 30 min (middle panel) and 60 min (right panel) renal sections. The upper panel represents the PAS-stained image and the lower panel represents the immunochemical-stained image with anti-NGAL antibody. Scale bars: 50 µm. (B) Graph comparing the tubular heights of sham, 30 min and 60 min. (C) Graph comparing the NGAL-positive area vs. total area of sham, 30 min and 60 min. Data are expressed as mean ± standard deviation; *P*-values were calculated by Bonferroni's multigroup test. (D) Scatter plots with liner regression show correlation analysis between the height of tubules height and NGAL-positive area. The linear regression line shows an inverse correlation between tubular height and NGAL-positive areas. Correlation coefficients *R* and *P* values are shown. Black circles indicate the sham group (*n*=3), black squares indicate the 30 min group (*n*=3), and black triangles indicate the 60 min group (*n*=3). **P*<0.05, ***P*<0.01

prominent at 4 weeks after ADR administration, whereas an intermediate condition between AKI and CKD is observed at less than 4 weeks [24]. In the present study, we assessed tubular flattening in mice 2 weeks after ADR treatment, an intermediate condition. The level of renal tubular injury was evaluated by measuring the expression of NGAL, which increases in the cells of damaged renal tubules [6]. Renal tubular heights were measured, and immunochemistry staining using an anti-NGAL antibody was performed on the renal tissues of the ADR and vehicle groups. No positive image of Sirius red staining was detected (data not shown). Tubular flattening was enhanced by ADR administration, and an evident increase in NGAL expression was demonstrated (Fig. 3A–C). In addition, linear regression analysis of tubular heights and NGAL expression levels showed an opposite correlation ($R^2=0.522$, $P=0.043$) (Fig. 3D).

DISCUSSION

Strong correlations between renal tubular flattening and interstitial fibrosis in severe CKD models and between tubular flattening and tubular disorder in ADR and IR models, were demonstrated in this study. There are various mechanisms by which glomerular lesions spread to interstitial fibrosis through tubular disorders. A study reported that renal tubule damage (flattening) induces interstitial fibrosis, the production of extracellular matrix (ECM), and inflammatory cell infiltration. The strong correlation between renal tubular flattening and renal tubular interstitial fibrillization observed in this study probably corresponds to the previously reported causal association; i.e., renal tubular damages induce fibrosis, ECM production, and cell infiltration. Another study also showed a correlation between enhanced NGAL expression and renal tubular atrophy (another renal disorder injury score item), with results similar to the renal tubular flattening score obtained in this study [26]. In this study, only male

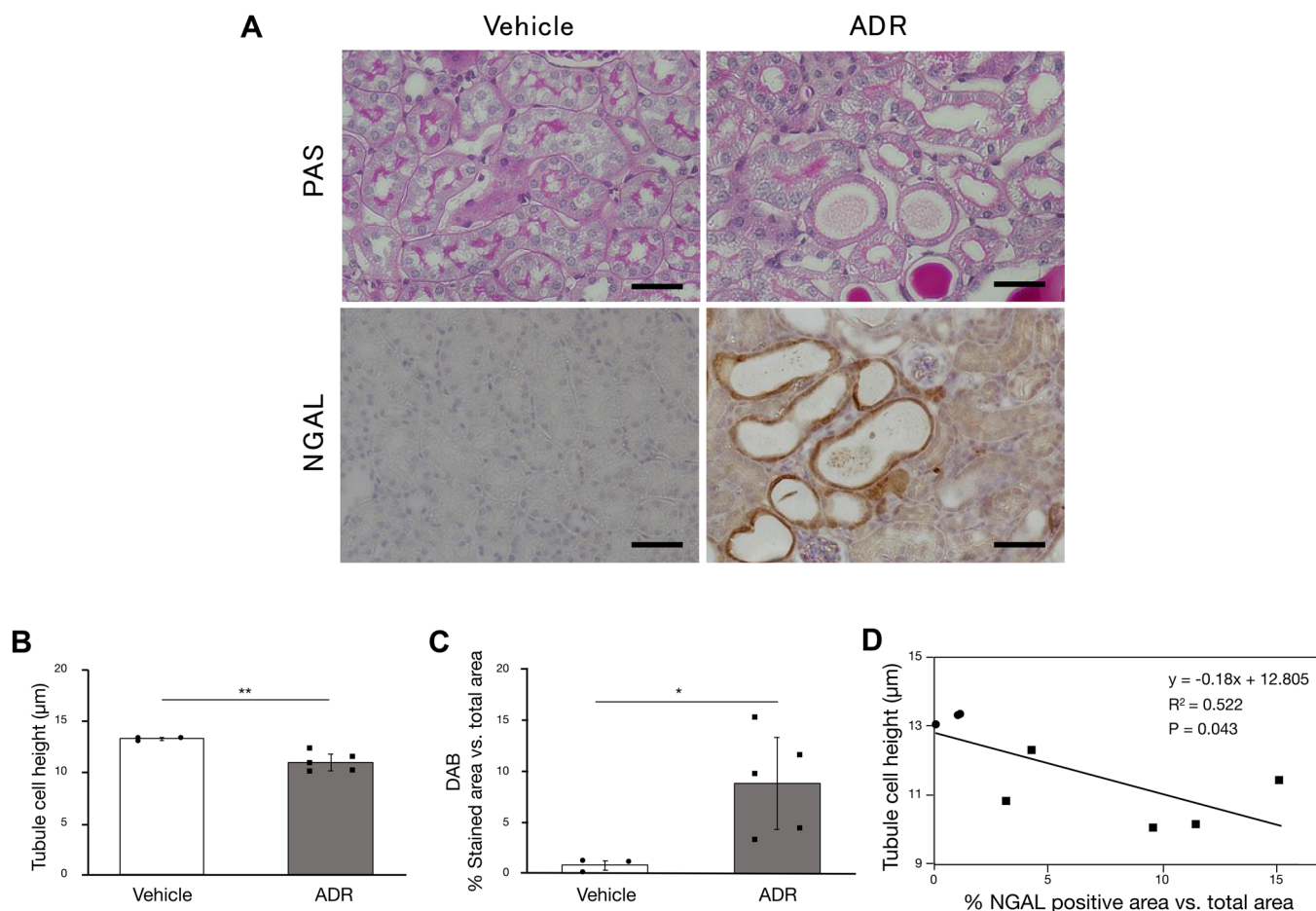


Fig. 3. (A) Representative images of Periodic Acid- Schiff (PAS) staining and immunochemical-stained images with anti- neutrophil gelatinase-associated lipocalin (NGAL) antibody of vehicle (left panel) and adriamycin (ADR) (right panel) renal sections. The upper panel represents the PAS-stained image and the lower panel represents the immunochemical-stained image with anti-NGAL antibody. Scale bars: 50 µm. (B) Graph comparing the tubular heights of vehicle and ADR. (C) Graph comparing the NGAL-positive area vs. total area. Data are expressed as mean ± standard deviation; *P*-values were calculated by Bonferroni’s multigroup test. (D) Scatter plots with liner regression show correlation analysis between the height of tubules and NGAL-positive area. The linear regression line shows an inverse correlation between tubular height and NGAL-positive areas. Correlation coefficients *R* and *P* values are shown. Black circles indicate the vehicle group (n=3), and black squares indicate the ADR group (n=5). **P*<0.05, ***P*<0.01.

mice were used, but flattening of tubules in nephropathy can be observed in both sexes. However, female mice have been reported to be resistant to IR and other nephropathy models, so the use of male or female mice should be considered depending on the nephropathy model used [8]. It was also difficult to assess tubular flattening in the medulla, because the tubules in the medulla at the time of non-injury have thin tubular cells, although the height of the tubules in the cortex was assessed. Therefore, a simple method to assess tubular injury in the medulla should be developed in the future (data not shown). Experts such as pathologists or clinicians generally perform an evaluation of the level of atrophy, expansion, or mutation of renal tubules to score the histology of renal tubules; however, the measurement of renal tubular heights to score the level of flattening can be performed much more easily compared with other methods. This is also advantageous because rapidly advancing technologies such as artificial intelligence and image processing can be easily applied; hence, a more precise, objective, and quantitative diagnosis should be possible in the future. To confirm whether renal tubular flattening could be a phenomenon that is universally observed as a CKD malignancy index across different species, further investigations using CKD models of other rodents, companion animals such as dogs and cats, or samples collected from humans should be conducted.

CONFLICT OF INTEREST. The authors have no conflicts of interest directly relevant to the content of this article.

ACKNOWLEDGMENTS. This work was supported by the Ministry of Education, Culture, Sports, Science and Technology (MEXT), Grant-in-Aid for Scientific Research, KAKENHI (16K16606) to H.S. and KAKENHI (20302614) to N.S.

REFERENCES

1. Baisantry, A., Bhayana, S., Rong, S., Ermeling, E., Wrede, C., Hegermann, J., Pennekamp, P., Sörensen-Zender, I., Haller, H., Melk, A. and Schmitt, R. 2016. Autophagy induces prosenescence changes in proximal tubular S3 segments. *J. Am. Soc. Nephrol.* **27**: 1609–1616. [[Medline](#)] [[CrossRef](#)]
2. Broekema, M., Harmsen, M. C., Koerts, J. A., Petersen, A. H., van Luyn, M. J. A., Navis, G. and Popa, E. R. 2005. Determinants of tubular bone marrow-derived cell engraftment after renal ischemia/reperfusion in rats. *Kidney Int.* **68**: 2572–2581. [[Medline](#)] [[CrossRef](#)]
3. Chen, J., You, H., Li, Y., Xu, Y., He, Q. and Harris, R. C. 2018. EGF receptor-dependent YAP activation is important for renal recovery from AKI. *J. Am. Soc. Nephrol.* **29**: 2372–2385. [[Medline](#)] [[CrossRef](#)]
4. Chou, A. H., Lee, C. M., Chen, C. Y., Liou, J. T., Liu, F. C., Chen, Y. L. and Day, Y. J. 2014. Hippocampal transcriptional dysregulation after renal ischemia and reperfusion. *Brain Res.* **1582**: 197–210. [[Medline](#)] [[CrossRef](#)]
5. Dong, Y., Zhang, Q., Wen, J., Chen, T., He, L., Wang, Y., Yin, J., Wu, R., Xue, R., Li, S., Fan, Y. and Wang, N. 2019. Ischemic duration and frequency determines AKI-to-CKD progression monitored by dynamic changes of tubular biomarkers in IRI mice. *Front. Physiol.* **10**: 153. [[Medline](#)] [[CrossRef](#)]
6. Di Grande, A., Giuffrida, C., Carpinteri, G., Narbone, G., Pirrone, G., Di Mauro, A., Calandra, S., Noto, P., Le Moli, C., Alongi, B. and Nigro, F. 2009. Neutrophil gelatinase-associated lipocalin: a novel biomarker for the early diagnosis of acute kidney injury in the emergency department. *Eur. Rev. Med. Pharmacol. Sci.* **13**: 197–200. [[Medline](#)]
7. Grande, M. T. and López-Novoa, J. M. 2009. Fibroblast activation and myofibroblast generation in obstructive nephropathy. *Nat. Rev. Nephrol.* **5**: 319–328. [[Medline](#)] [[CrossRef](#)]
8. Hu, H., Wang, G., Batteux, F. and Nicco, C. 2009. Gender differences in the susceptibility to renal ischemia-reperfusion injury in BALB/c mice. *Tohoku J. Exp. Med.* **218**: 325–329. [[Medline](#)] [[CrossRef](#)]
9. Ichimura, T., Asselton, E. J. P. V., Humphreys, B. D., Gunaratnam, L., Duffield, J. S. and Bonventre, J. V. 2008. Kidney injury molecule-1 is a phosphatidylserine receptor that confers a phagocytic phenotype on epithelial cells. *J. Clin. Invest.* **118**: 1657–1668. [[Medline](#)] [[CrossRef](#)]
10. Kamijo-Ikemori, A., Ichikawa, D., Matsui, K., Yokoyama, T., Sugaya, T. and Kimura, K. 2013. [Urinary L-type fatty acid binding protein (L-FABP) as a new urinary biomarker promulgated by the Ministry of Health, Labour and Welfare in Japan]. *Rinsho Byori* **61**: 635–640 (in Japanese). [[Medline](#)]
11. Kirihara, Y., Takechi, M., Kurosaki, K., Kobayashi, Y. and Kurosawa, T. 2013. Anesthetic effects of a mixture of medetomidine, midazolam and butorphanol in two strains of mice. *Exp. Anim.* **62**: 173–180. [[Medline](#)] [[CrossRef](#)]
12. Ko, G. J., Grigoryev, D. N., Linfert, D., Jang, H. R., Watkins, T., Cheadle, C., Racusen, L. and Rabb, H. 2010. Transcriptional analysis of kidneys during repair from AKI reveals possible roles for NGAL and KIM-1 as biomarkers of AKI-to-CKD transition. *Am. J. Physiol. Ren. Physiol.* **298**: 1472–1483. [[CrossRef](#)]
13. Lee, V. W. and Harris, D. C. 2011. Adriamycin nephropathy: a model of focal segmental glomerulosclerosis. *Nephrology (Carlton)* **16**: 30–38. [[Medline](#)] [[CrossRef](#)]
14. Levey, A. S., Atkins, R., Coresh, J., Cohen, E. P., Collins, A. J., Eckardt, K. U., Nahas, M. E., Jaber, B. L., Jadoul, M., Levin, A., Powe, N. R., Rossert, J., Wheeler, D. C., Lameire, N. and Eknoyan, G. 2007. Chronic kidney disease as a global public health problem: approaches and initiatives - a position statement from kidney disease improving global outcomes. *Kidney Int.* **72**: 247–259. [[Medline](#)] [[CrossRef](#)]
15. Levin, A., Stevens, P. E., Bilous, R. W., Coresh, J., Francisco, A. L. M. De, Jong, P. E. De, Griffith, K. E., Hemmelgarn, B. R., Iseki, K., Lamb, E. J., Levey, A. S., Riella, M. C., Shlipak, M. G., Wang, H. T. C. and Winearls, C. G. 2013. Kidney disease: Improving global outcomes (KDIGO) CKD work group. KDIGO 2012 clinical practice guideline for the evaluation and management of chronic kidney disease. *Kidney Int. Suppl.* **3**: 1–150.
16. Mishra, J., Ma, Q., Prada, A., Mitsnefes, M., Zahedi, K., Yang, J., Barasch, J. and Devarajan, P. 2003. Identification of neutrophil gelatinase-associated lipocalin as a novel early urinary biomarker for ischemic renal injury. *J. Am. Soc. Nephrol.* **14**: 2534–2543. [[Medline](#)] [[CrossRef](#)]
17. Sasaki, H., Marusugi, K., Kimura, J., Kitamura, H., Nagasaki, K., Torigoe, D., Agui, T. and Sasaki, N. 2015. Genetic background-dependent diversity in renal failure caused by the *tenis2* gene deficiency in the mouse. *Biomed. Res.* **36**: 323–330. [[Medline](#)] [[CrossRef](#)]
18. Skrypnik, N. I., Harris, R. C. and de Caestecker, M. P. 2013. Ischemia-reperfusion model of acute kidney injury and post injury fibrosis in mice. *J. Vis. Exp.* **78**: 50495. [[Medline](#)]
19. Stoyanoff, T. R., Todaro, J. S., Aguirre, M. V., Zimmermann, M. C. and Brandan, N. C. 2014. Amelioration of lipopolysaccharide-induced acute kidney injury by erythropoietin: involvement of mitochondria-regulated apoptosis. *Toxicology* **318**: 13–21. [[Medline](#)] [[CrossRef](#)]
20. Stoyanoff, T. R., Rodríguez, J. P., Todaro, J. S., Colavita, J. P. M., Torres, A. M. and Aguirre, M. V. 2018. Erythropoietin attenuates LPS-induced microvascular damage in a murine model of septic acute kidney injury. *Biomed. Pharmacother.* **107**: 1046–1055. [[Medline](#)] [[CrossRef](#)]
21. Takahashi, Y., Sasaki, H., Okawara, S. and Sasaki, N. 2018. Genetic loci for resistance to podocyte injury caused by the *tenis2* gene deficiency in mice. *BMC Genet.* **19**: 24. [[Medline](#)] [[CrossRef](#)]
22. Uchio-Yamada, K., Monobe, Y., Akagi, K., Yamamoto, Y., Ogura, A. and Manabe, N. 2016. *Tenis2*-deficient mice on FVB/N background develop severe glomerular disease. *J. Vet. Med. Sci.* **78**: 811–818. [[Medline](#)] [[CrossRef](#)]
23. Vaidya, V. S., Ferguson, M. A. and Bonventre, J. V. 2008. Biomarkers of acute kidney injury. *Annu. Rev. Pharmacol. Toxicol.* **48**: 463–493.
24. Wang, Y., Wang, Y. P., Tay, Y. C. and Harris, D. C. H. 2000. Progressive adriamycin nephropathy in mice: sequence of histologic and immunohistochemical events. *Kidney Int.* **58**: 1797–1804. [[Medline](#)] [[CrossRef](#)]
25. Wright, J. R., Duggal, A., Thomas, R., Reeve, R., Roberts, I. S. D. and Kalra, P. A. 2001. Clinicopathological correlation in biopsy-proven atherosclerotic nephropathy: implications for renal functional outcome in atherosclerotic renovascular disease. *Nephrol. Dial. Transplant.* **16**: 765–770. [[Medline](#)] [[CrossRef](#)]
26. Wu, Y., Yang, L., Su, T., Wang, C., Liu, G. and Li, X. M. 2010. Pathological significance of a panel of urinary biomarkers in patients with drug-induced tubulointerstitial nephritis. *Clin. J. Am. Soc. Nephrol.* **5**: 1954–1959. [[Medline](#)] [[CrossRef](#)]
27. Zheng, M., Cai, J., Liu, Z., Shu, S., Wang, Y., Tang, C. and Dong, Z. 2019. Nicotinamide reduces renal interstitial fibrosis by suppressing tubular injury and inflammation. *J. Cell. Mol. Med.* **23**: 3995–4004. [[Medline](#)] [[CrossRef](#)]